Plasmonic Modes Revealed

Philip E. Batson

Science **335**, 47 (2012);
DOI: 10.1126/science.1215588

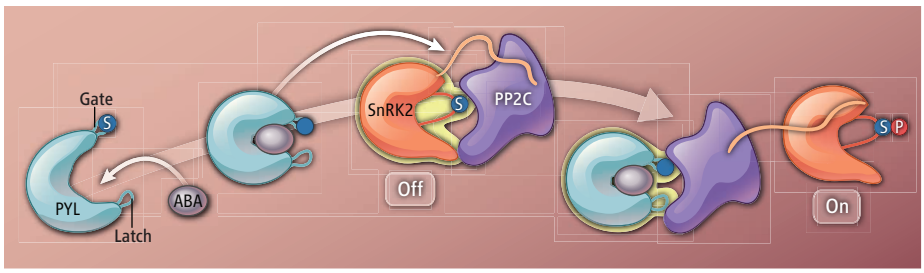

Partner swap. Molecular mimicry between the kinase SnRK2 and the hormone receptor PYL bound to ligand ABA permits alternate binding to the PP2C phosphatase. This change in partners activates (on) or deactivates (off) SnRK2, allowing it to phosphorylate downstream signals.

serine in the activation loop of SnRK2.6, the binding further suppresses any remaining kinase activity. To uncloak the details of this two-step mechanism, a fusion protein HAB1-SnRK2.6 was generated as a linear peptide. By incorporating entropy-decreasing mutations, the authors coaxed the fused protein into high-quality crystals. Structural analysis of the complex revealed that the kinase SnRK2.6 mimicks the face of the ABA receptor that binds to the phosphatase HAB1. The major contact surface between this kinase and phosphatase runs along their catalytic sites. Like the "gate" structure of the ABA receptor in the ABA-PYL-PP2C complex, the activation loop of the kinase SnRK2.6 also inserts into the catalytic center of the phosphatase HAB1. The cleft between the "gate" and "latch" of the receptor is also mimicked by a pocket in the C-lobe region of SnRK2.6. The contact between the αG helix of SnRK2.6 and a loop structure in HAB1 is adjacent to the HAB1 Trp^{385}-PYL interaction loop. Thus, the receptor, once bound by ABA, adopts a surface structure remarkably similar to that of the kinase (see the figure).

ABA-PYL-PP2C and the SnRK2-PP2C complexes are not mutually exclusive as expected. ABA-PYL-SnRK2-PP2C in fact forms a quaternary complex. This is because, in addition to the kinase catalytic domain, a second acidic motif of ~25 residues called the ABA box found in the C terminus of SnRK2.2, SnRK2.3, and SnRK2.6 can also interact with HAB1 (but not with the receptors). The other seven SnRK2 members in the family have no obvious ABA box, but the overall amino acid compositions in the coincidental regions are acidic. With the exception of two SnRK2 enzymes, each of the other five acidic motifs also interacts with a subset of the PP2Cs. HAB1 can bridge the interaction between the receptor PYL2 and SnRK2.6 in the presence of ABA, but not in its absence. This means that the ABA-bound receptor can dislodge the kinase from the phosphatase without fully dissociating these two proteins; the kinase will remain tethered by its ABA box to the phosphatase. This also explains why the PYL2-HAB1 complex can be disrupted by using increasing concentrations of the isolated kinase domain of SnRK2.6, whereas the ABA-bound receptors cannot dissociate SnRK2-PP2C, even if the ABA-bound receptors have much stronger affinity for the phosphatases relative to the kinases.

Soon *et al*. hint that molecular mimicry might be a common mechanism in many biological processes involving kinase-phosphatase complexes. Tantalizing parallels can be found in the catalytically inactive pseudophosphatases EGG-4 and EGG-5 in mammals, which recognize the activation loop of the kinase MBK-2 and block its kinase activity. The mammalian AMPK-PP2Cα complex (homologs of the SnRKs and PP2Cs of *Arabidopsis*) might also pack their catalytic sites to maintain the kinase inactive. The structural studies on the core ABA signaling proteins establish a new paradigm for kinase-phosphatase co-regulation and coevolution. Indeed, subversion and deception by competitive binding of these major cell signaling proteins in biasing important biological decisions may turn out to be pervasive.

References

1. F.-F. Soon *et al*., *Science* **335**, 85 (2012); 10.1126/science.1215106.
2. S. R. Cutler, P. L. Rodriguez, R. R. Finkelstein, S. R. Abrams, *Annu. Rev. Plant Biol.* **61**, 651 (2010).
3. H. Fujii *et al*., *Nature* **462**, 660 (2009).
4. A. Joshi-Saha, C. Valon, J. Leung, *Sci. Signal.* **4**, re4 (2011).
5. T. Umezawa *et al*., *Proc. Natl. Acad. Sci. U.S.A.* **106**, 17588 (2009).
6. F. Vlad *et al*., *Plant Cell* **21**, 3170 (2009).
7. S.-Y. Park *et al*., *Science* **324**, 1068 (2009); 10.1126/science.1173041.
8. H. Fujii, J.-K. Zhu, *Proc. Natl. Acad. Sci. U.S.A.* **106**, 8380 (2009).
9. R. Yoshida *et al*., *J. Biol. Chem.* **281**, 5310 (2006).
10. N. Nishimura *et al*., *Plant J.* **61**, 290 (2010).

10.1126/science.1217667

APPLIED PHYSICS

Plasmonic Modes Revealed

Philip E. Batson

Time-resolved electron microscopy can map the electric field created in and around a nanoparticle by photonic excitation of its plasmonic modes.

When nanostructures made of metals such as gold and silver are illuminated with visible light, plasmonic modes can be excited that cause conduction electrons to oscillate. This motion creates a pattern of electric fields, extending both within and outside the structure, that can be tuned by changing the particle size and shape to efficiently couple light to electronic processes. Practical applications of this coupling include improved harvesting of light for photovoltaics (*1*) and enhanced sensitivity for sensors based on light-emitting messenger molecules (*2*). Although there is well-developed theoretical understanding of how photons interact with nanostructures that are much smaller than their wavelength, we have few methods for measuring electric fields nearby and within nanoscale structures during photonic excitation. On page 59 of this issue, Yurtsever *et al*. (*3*) report using time-resolved electron energy gain/loss spectroscopy in an electron microscope to obtain spatially resolved maps of electric fields that result when nanoscale metal objects are illuminated by incident photons.

Previously, optically induced plasmonic electric fields have been probed by near-field scanning optical microscopy (NSOM) and its variants that use metal tips (*4*, *5*). In NSOM, a subwavelength optical aperture samples photon intensity as a function of position. However, spatial resolution and collection efficiency are both limited because NSOM samples only the decaying or evanescent part of the optical signal outside the nanoscale object.

Institute for Advanced Materials, Devices and Nanotechnology, Rutgers University, Piscataway, NJ 08854, USA. E-mail: batson@physics.rutgers.edu

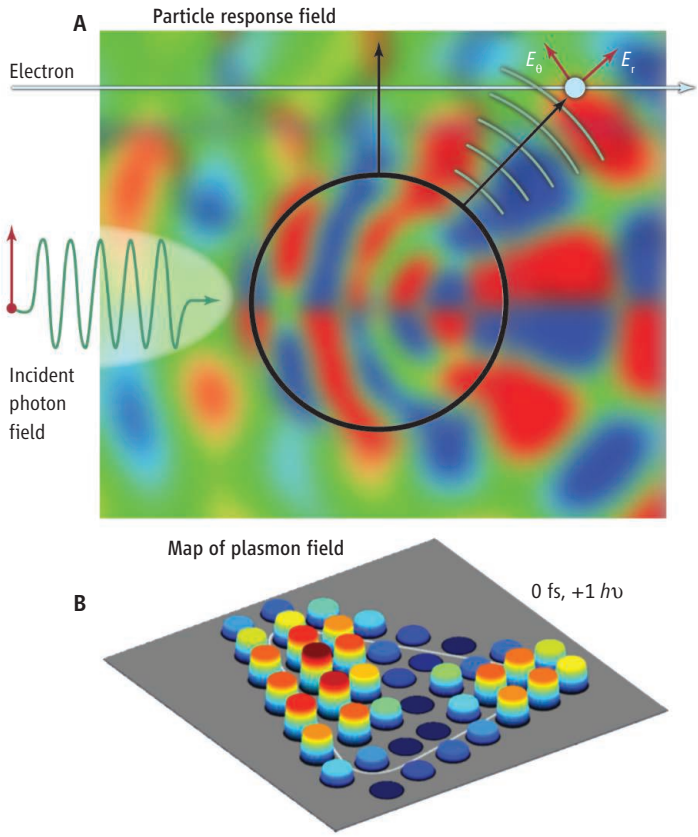

Field day for plasmons. (**A**) The theoretical basis for the experiment of Yurtsever *et al*. is shown. A kiloelectron-volt electron interacts with the evanescent electric field created by a photon exciting a metal nanocylinder (shown in cross section). Blue and red colors indicate the phase of the plasmon response field E_θ and E_r; near-zero responses are in green. Depending on the arrival time of the electron, it can gain or lose energy by interacting with this field. [Adapted from (*14*)] (**B**) A map of the intensity of electron energy gain as a function of position on a triangular nanoscale silver particle. The map integrates scattering through or past the nanoparticle, along the electron trajectory.

Electron energy-loss scattering can also efficiently create surface plasmon modes within groups of nanoscale metal objects, allowing spatial investigation of resonant plasmonic response. This technique supported understanding of surface-enhanced Raman scattering on silver surfaces with nanoscale roughness, and suggested interesting possibilities for engineering optical coupling to nanoscale systems (*6*, *7*). The possibility of deliberate acceleration of electrons by light, mediated by gratings and surface-guided modes to match the momentum transfer required by electrons (*8*, *9*), has also been considered. Finally, electron energy-gain spectroscopy might combine nanoscale spatial resolution with the energy selectivity of photons (*10*).

Observation of electron energy gain has had little success, however, apparently because of the difficulty of coupling enough light into the nanoscale object so that each incident electron would have sufficiently high probability for interaction with plasmonic fields. Electron-beam currents in electron microscopy are so small that only about one electron per nanosecond interacts with the specimen, whereas plasmon decay happens on the femtosecond time scale, producing a timing mismatch of five orders of magnitude. Thus, electron energy-loss events that create a plasmon and scatter the electron simultaneously are quite common, whereas energy-gain events, which require absorption of a separately created plasmon, have not been observed previously.

During the past few years, Zewail's group (*11*) and others (*12*, *13*) have introduced laser-excited photocathodes to electron microscopy, enabling time-resolved experiments. It is now possible to optically excite or "pump" the specimen and then probe it with an electron at a later time. Yurtsever *et al*. convincingly demonstrate a direct interaction of high-energy electrons with surface plasmon fields excited by incident photons in single nanostructures. A theoretical model developed by Park *et al*. summarizes the experiment (*14*) (see the figure, panel A). In this case, the nanostructure is a metal cylinder (depicted as a circle, with its axis perpendicular to the page). A photon field incident from the left excites surface plasmons, producing response fields both inside and outside the cylinder. These fields are summarized by the background image, with red or blue colors denoting positive or negative phase of the response field. A high-energy electron is incident from the left, and, depending on the particular timing of its arrival, can be either accelerated or decelerated by the fields, providing energy gain or loss. In this illustration, the electron passes outside the cylinder, sampling evanescent fields beyond the cylinder surface.

In a semiclassical treatment, the electron is represented by a point charge, and the total energy gain or loss is determined by an integral over its path (*15*). The timing accuracy of the electron's arrival is limited to a few hundred femtoseconds by the laser and pulse width, as well as by the instrumental details of the electron photogeneration and acceleration. Thus, electrons arrive during a spread of times around the arrival of the photon field, producing energy gain or loss, depending on the details of the surface plasmon response phase during the electron passage. If the response field is very strong, multiple quanta of energy can be transferred to or from the electron. In the case of a single triangular silver nanoparticle, many electrons undergo no loss, but some gain or lose one or two quanta of energy. The energy gain and loss peaks are exceptionally strong—several times the electron energy-loss scattering probability in the absence of the incident photon.

With such a strong set of energy gain and loss peaks, Yurtsever *et al*. produced maps of field intensity inside and outside nanoscale objects. An example for the energy gain of $+h\nu$ at a time delay of 0 fs from the triangular silver nanoparticle is shown in panel B of the figure. In scattering near the surface of copper, peaks situated at many discrete energy quanta were also evident. The experimental visualization of the optical response of a nanoscale dielectric object will be important for many applications, including renewable energy sources, continued scaling of semiconductor computation capabilities, and understanding of dielectric structures that exhibit unusual properties.

References

1. A. Aubry *et al*., *Nano Lett.* **10**, 2574 (2010).
2. N. Liu, M. L. Tang, M. Hentschel, H. Giessen, A. P. Alivisatos, *Nat. Mater.* **10**, 631 (2011).
3. A. Yurtsever, R. M. van der Veen, A. H. Zewail, *Science* **335**, 59 (2012).
4. E. Betzig, A. Lewis, A. Harootunian, M. Isaacson, E. Kratschmer, *Biophys. J.* **49**, 269 (1986).
5. Y. Inouye, S. Kawata, *Opt. Lett.* **19**, 159 (1994).
6. P. E. Batson, *Phys. Rev. Lett.* **49**, 936 (1982).
7. P. E. Batson, *Surf. Sci.* **156**, 720 (1985).
8. S. J. Smith, E. M. Purcell, *Phys. Rev.* **92**, 1069 (1953).
9. K. Mizuno, J. Pae, T. Nozokido, K. Furuya, *Nature* **328**, 45 (1987).
10. F. J. García de Abajo, M. Kociak, *New J. Phys.* **10**, 073035 (2008).
11. A. H. Zewail, *Science* **328**, 187 (2010).
12. H. Dömer, O. Bostanjoglo, *Appl. Surf. Sci.* **208–209**, 442 (2003).
13. J. S. Kim *et al*., *Science* **321**, 1472 (2008).
14. S. T. Park, M. M. Lin, A. H. Zewail, *N. J. Phys.* **12**, 123028 (2010).
15. R. H. Ritchie, *Phys. Rev.* **106**, 874 (1957).

10.1126/science.1215588

Published by AAAS